A R C H I V E S O F M E T A L L U R G Y A N D M A T E R I A L S
Volume 58 2013 Issue 1
DOI: 10.2478/v10172-012-0156-7

R. WŁODARCZYK*, A. WROŃSKA**

EFFECT OF pH ON CORROSION OF SINTERED STAINLESS STEELS USED FOR BIPOLAR PLATES IN POLYMER EXCHANGE MEMBRANE FUEL CELLS

WPŁYW pH ROZTWORU NA SZYBKOŚĆ KOROZJI SPIEKANYCH STALI NIERDZEWNYCH STOSOWANYCH NA OKŁADKI OGNIW PALIWOWYCH Z MEMBRANĄ POLIMEROWĄ

Proton exchange membrane fuel cells (PEMFCs) are numbered among low-temperature cells. Their operating temperature reaches 120°C, whereas their efficiency amounts to ca. 40%. These cells are most often used for the batteries for portable devices, low and high power generators, stationary power plants and car drives. The PEMFCs are composed of the membrane, electrodes at both sides and bipolar plates, also termed interconnectors.

The main aim of the present study was to investigate the sintered stainless steels in simulated environments of a PEM fuel cells for bipolar plates. The ferritic (434L) and austenitic (316L) stainless steels were examined. The corrosion properties were examined in 0.1 mol dm^{-3} Na_2SO_4+ 2 ppmF^- (pH= 1; 3; 5) at 80°C.

Keywords: fuel cell, bipolar plates, corrosion, sintered stainless steel, structural analysis, corrosion resistance

Ogniwa paliwowe z membraną protonowymienną są jednym, z niskotemperaturowych ogniw. Ich temperatura pracy wynosi 120°C, a sprawność dochodzi do 40%. Tego typu ogniwa są najczęściej używane jako generatory do urządzeń przenośnych, małych i średnich stacjonarnych elektrowni i do napędu samochodowego. Ogniwa PEMFC (Proton Exchange Membrane Fuel Cell) składają się z membrany, elektrod po obu jej stronach oraz okładek, nazywanych też interkonektorami. Głównym celem niniejszej pracy było zbadanie spiekanych stali nierdzewnych przeznaczonych na okładki, w symulowanych środowiskach ogniw paliwowych PEMFC. Badano stal ferrytyczną (434L) oraz austenityczną (316L). Odporność korozyjna stali badano w 0.1 mol dm^{-3} Na_2SO_4+2 ppmF^- (pH= 1; 3; 5) w temperaturze 80°C.

1. Introduction

Fuel cells constitute generators which produce electricity and heat as a result of chemical reactions which occurred in electrodes [1]. In typical fuel cells, production of energy consists in flameless combustion of the continuously supplied fuel (hydrogen) in the presence of oxidant (oxygen). As a result of chemical reactions, oxygen is reduced and produces water. Oxidation of hydrogen occurs in anode. Protons, which are created as a result of this reaction, permeate through the ion-exchange membrane / electrolyte and are used in the reaction of oxygen reduction (cathode) (Fig. 1) [2]. Media are supplied to the electrodes through channels in bipolar plates (BPs). It is even distribution of media in the surface of electrodes which determines (among other things) the efficiency of fuel cells.

Among many solutions to generate energy, use of fuel cells to generate electricity and heat should be emphasised [1-2]. Fig. 1 presents the model of fuel cell with cylindrical electrodes. As can be observed from Fig. 1, single fuel cell is composed of the anode, cathode and electrolyte/membrane located between them.

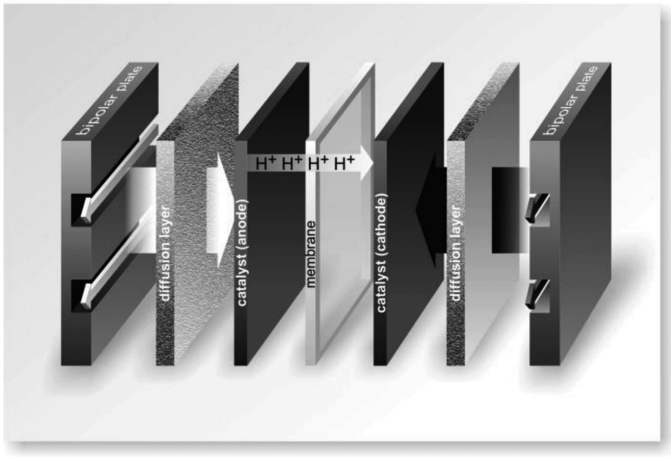

Fig. 1. Proton exchange membrane fuel cell

Bipolar plates must conduct electricity and be mechanically and chemically stable, made of low permeability materials, show corrosion resistance, allow for uniform distribution of reactant gas and product removal, be of low cost and able to be easy machined or shaped [3]. For transportation purposes,

* DEPARTMENT OF ENERGY ENGINEERING, DEPARTMENT OF ENVIRONMENTAL ENGINEERING AND BIOTECHNOLOGY, CZĘSTOCHOWA UNIVERSITY OF TECHNOLOGY, 42-200 CZĘSTOCHOWA, 60A BRZEŹNICKA STR., POLAND
** INSTITUTE OF MATERIALS ENGINEERING, CZĘSTOCHOWA UNIVERSITY OF TECHNOLOGY, 42-200 CZĘSTOCHOWA, 60A BRZEŹNICKA STR., POLAND

lightweight and low volume should be also considered. First prototypes of fuel cells contained interconnectors made of graphite, which is material that meets the abovementioned requirements, yet expensive and difficult to be processed. Therefore, use of graphite on a wider scale disqualifies this material. An alternative for materials for bipolar plates can be provided by carbon composite materials [4], metals non-coated and coated with thin layers [5-6], Fe-based alloys and stainless steels [7-10]. Obviously, stainless steel plates are strongly recommended due to their relatively high strength, high chemical stability, wide range of choice, simplicity of mass production and low cost.

The subject of the present study is sintered stainless steels, which are expected to be perfect materials for fuel cells. Application of powder metallurgy allows for suitable selection of the powder grain size and composition. Optimization of chemical and mechanical properties can be achieved through selection of the parameters of compaction and sintering (temperatures, compaction pressures and the atmosphere of sintering). Furthermore, properly designed die for sinter compaction allows for cheap and fast manufacturing of parts of fuel cells. Natural porosity of sinters is likely to meet fundamental requirement imposed on interconnectors i.e. even distribution of media on the surface of electrodes. Materials designed for BPs must be characterized by a suitable corrosion resistance. Through the hydrogen ions produced during cell's operation, the environment is acidified, which causes intensification of the processes of degradation of metallic materials. Rise in aggressiveness of the environment is also connected with presence of ions from membrane i.e. F^-, SO_3^-, SO_4^- [11]. Products of corrosion of BPs might poison the catalysts and decrease the efficiency of the fuel cell.

The main aim of the present study was to investigate the sintered stainless steels in simulated environments of PEM fuel cells. Ferritic (434L) and austenitic (316L) stainless steels were examined. The corrosion properties were examined in 0.1 mol dm^{-3} Na_2SO_4+ 2 ppmF^- (pH= 1, 3, 5) at 80°C.

2. Experimental Part

2.1. Materials

Manufacturing of bipolar plates in fuel cells by means of powder metallurgy consisted in preparation of the powders and their mixtures and then cold-forming and sintering at the temperature of 1250°C for 30 min. in ammonia medium. Chemical composition of water-atomized powders of steels are presented in Table 1.

TABLE 1
Chemical composition of the powders used for sintering

Powder Grade	C [%]	Mo [%]	Ni [%]	Cr [%]	Si [%]	Mn [%]	Fe [%]
316LHD	0.025	2.2	12.3	16.7	0.9	0.1	balance
434 LHC	0.015	0.98	–	16.2	0.8	0.1	balance

The following sinters were obtained from the powders with grain size of 50μm:

- 100% 316L – sintered at the pressure of 700 MPa,
- 100% 434L – sintered at the pressure of 765 MPa,
- 50% 316L + 50% 434L – sintered at the pressure of 720 MPa.

Properties of the obtained sinters are presented in Table 2.

TABLE 2
Density of the obtained sinters

Material	Sinter density [g cm^{-3}]
100% 316L	6.70
100% 434L	6.60
50% 316L + 50% 434L	6.68

3. Methods

The samples were tested in Axiovert optical microscope. Phase analysis was conducted using XRD Seifert 3003 T-T X-ray diffractometer with radiation of $K_{\alpha Co}$-0.17902 nm.

Electrochemical measurements were carried out in three-electrode arrangement by means of CH Instrument unit. Reference electrode was formed by saturated calomel electrode (SCE) while auxiliary electrode was platinum wire. Working electrode was formed by the sintered materials. Measurements were taken in the solution of SO_4^{2-}+ 2ppm F^- o pH=1; pH= 3; pH= 5, at 80°C. Before electrochemical measurements were started, the samples had been polished with sandpaper. Potentiokinetic curves were recorded within the range of potentials from -0.7V to 1.6V vs. SCE, scan rate 5 mV s^{-1}. Among the curves recorded for the given material and environment, the most representative curves were selected for the analysis. On the basis of polarization curves, the parameters which define corrosion resistance of the material were determined, i.e. corrosion potential E_{corr}, density of corrosion current i_{corr}, polarization resistance R_p [10]. The corrosion current was determined by the Tafel-extrapolation method. This method is quicker than the method of direct measurement of the weight loss of the corrosion metal. In order to obtain the polarization resistance, the slope of the line ΔE =f(Δi) was measured.

Open circuit potential tests were used to measure the free corrosion potential in the different environments; in solution Na_2SO_4+ 2ppm F^- o pH=1; pH= 3; pH= 5, at 80°C.

4. Test Results and Discussion

4.1. Structural Analysis

Microstructure analysis revealed visible, irregular pores which were unevenly distributed throughout the material. Microstructure analysis for sintered 316L steel revealed austenitic structure with distinctive deformation twins, and the 434 LHC steel ferritic structure with martensite. Sintering of 316L steel with 434L steel in 50-50 ratio allowed for obtaining a material with multi-phase austenitic-ferritic-martenzitic structure (Fig. 2). Microstructural observations were confirmed with X-ray phase investigations (Fig. 3).

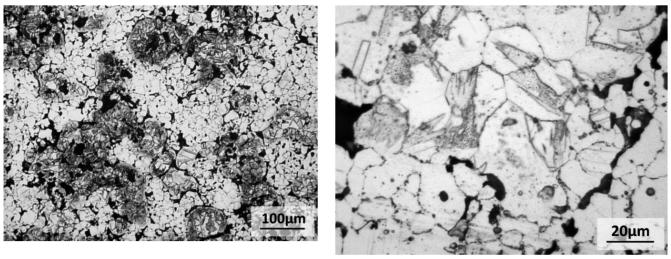

Fig. 2. Microstructure in sinter 50% 316L + 50% 434L

Based on the analysis of phase composition in the sinter 100% 316L, austenitic phase of FeCrNi, crystallizing in cubic body-centered cell with a=3.591 nm. In the case of 100% 434L sinter, Fe-α phase was observed. In the case of 50% 316L + 50% 434L sinter, the presence of ferritic and austenitic phase was confirmed. Because martensitic phase shows angular directions similar to ferritic phase, it was impossible to confirm its presence with X-ray investigations (martensitic phase was confirmed with microstructure testing).

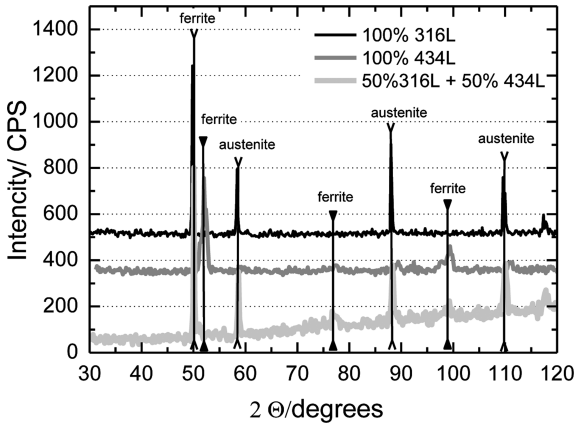

Fig. 3. Diffractograms of the examined sintered steels

4.2. Electrochemical Analysis

In order to determine the effect of solution pH on intensity of corrosion processes, polarization curves were registered for austenitic sinter of 100% 316L in the solution of Na_2SO_4+ 2 ppmF^-, at the temperature of 80°C (Fig. 4). The values of anode and cathode potentials under operating conditions of PEMFC were plotted on the chart. This potential is in the passive region for almost all the materials tested (except for multiphase materials, Fig. 6). A region of active solubilisation, passivation and transpassivation can be separated in polarization curves, whereas the curves registered in the solution with pH = 3 and pH = 5, are in fact identical. In the curve recorded in the environment with lowest pH, a shift of corrosion potential towards positive values was observed. Aggressiveness of this environment is proved by high corrosion current density of 2.56 mA cm^{-2} (polarization resistance amounts to 25.89 Ω cm^2) as compared to the other environments, where i_{corr} amounts to ca. 0.09 mA cm^{-2}, and polarization resistance ranged from 465.40 to 662.91 Ω cm^2. Values of the parameters assessed based on polarization curves are presented in Table 3.

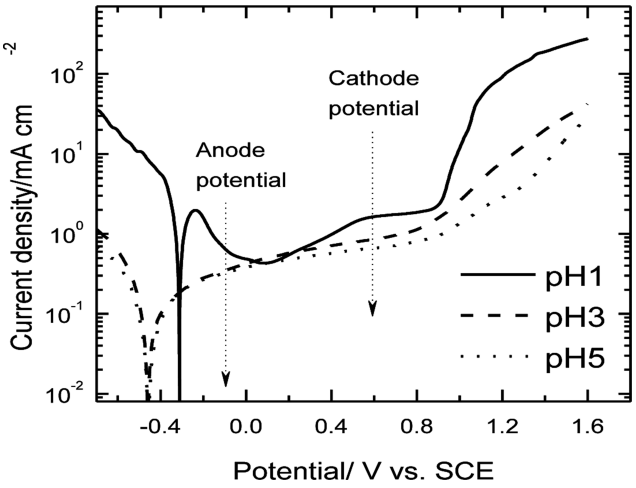

Fig. 4. Potentiokinetic curves obtained for 100%316L sinter

Effect of pH in solution on corrosion resistance in ferritic sinter is presented in Fig. 5. Comparison of the patterns of polarization curves reveals that the value of potential corrosion does not depend on pH of solution. The value of corrosion current density in low pH was almost three orders of magnitude higher (11.42 mA cm^{-2}) as compared to the value of i_{corr} assessed for solutions with higher pH (i_{corr} = 0.06 mA cm^{-2} for the solution with pH = 3; i_{corr} = 0.04 mA cm^{-2} for pH = 5). No considerable differences in the patterns of polarization curves in solutions of pH = 3 and pH = 5.

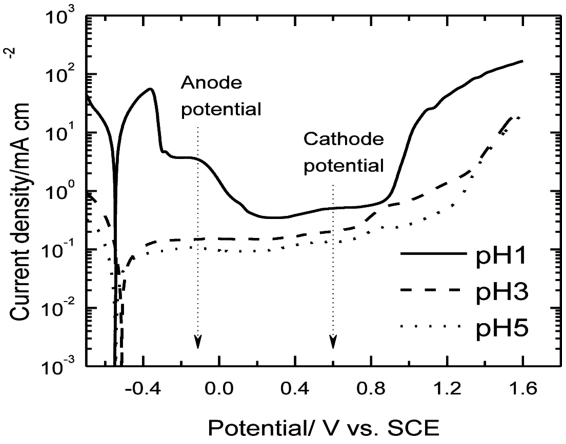

Fig. 5. Potentiokinetic curves obtained for 100%434L sinter

In consideration of applications of sintered materials, it should be noted both austenitic 316L sinter and the sinter with ferritic structure (434L) show high values of current densities for the potentials which correspond to operating anode and cathode conditions. High values of currents combined with low polarization resistance do not allow for application of these materials for bipolar plates in PEMs. In consideration of fundamental requirements imposed on the materials for bipolar plates in fuel cells, the sinter with multiphase structure was proposed. Fig. 6 presents polarization curves recorded for 50% 316L + 50% 434L sinter. The value of corrosion potential in the sinter changes in relation to pH in the solution. Similar sequence was observed for the value of i_{corr}: higher pH values correspond to the value of E_{corr} and higher values of i_{corr}. Comparison of the values of polarization resistance assessed for the multiphase sinter to 316L and 434L sinter

revealed that the highest resistance to corrosion was obtained in each of the studied environments (Table 3).

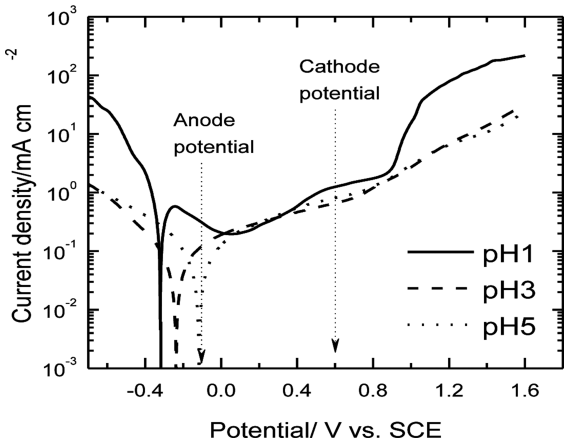

Fig. 6. Potentiokinetic curves obtained for 50%316L + 50%434L sinter

TABLE 3
Electrochemical parameters from polarization curves

Materials	Parameters	pH = 1	pH = 3	pH = 5
100% 316L	E_{corr} [V]	-0.302	-0.458	-0.467
	i_{corr} [mA cm^{-2}]	2.561	0.094	0.067
	R_p [Ω cm^2]	25.89	465.40	662.91
100% 434L	E_{corr} [V]	-0.541	-0.519	-0.537
	i_{corr} [mA cm^{-2}]	11.42	0.066	0.044
	R_p [Ω cm^2]	3.01	538.26	891.85
50% 316L + 50% 434L	E_{corr} [V]	-0.328	-0.242	-0.112
	i_{corr} [mA cm^{-2}]	0.508	0.079	0.102
	R_p [Ω cm^2]	75.97	912.14	863.86

According to Stern-Hoar's equation, the value of density of external current changes linearly in relation to potential within the potential ranges which do not considerably differ from corrosion potential (±20mV). The slope of the line of ΔE =f(Δi) is a measure of polarisation resistance: the higher value of polarization resistance, the higher material's resistance to corrosion in the given environment. Based on the data presented in Fig. 4-6, the diagram for the relationship between the changes in the value of external current as a function of the voltage was prepared. Fig. 7 presents the relationship prepared based on polarization curves recorded for each material in the solution of pH=1. The same method was used for the relationship determined based on potentiokinetic curves in the solutions with pH = 3 and pH = 5 (not presented in this paper).

Fig. 8 presents open circuit potential versus time for sintered stainless steel in different environments. Comparison of the registered curves reveals that, regardless of pH of the solution, the lowest value of potential can be observed for 316L austenitic sinter. The sinter with multiphase structure shows highest potential values. It is generally accepted that higher potential means that corrosion is retarded. Therefore, we can say that at free corrosion potential, best corrosion resistance can be observed for the sinter of 50% 316L + 50% 434L.

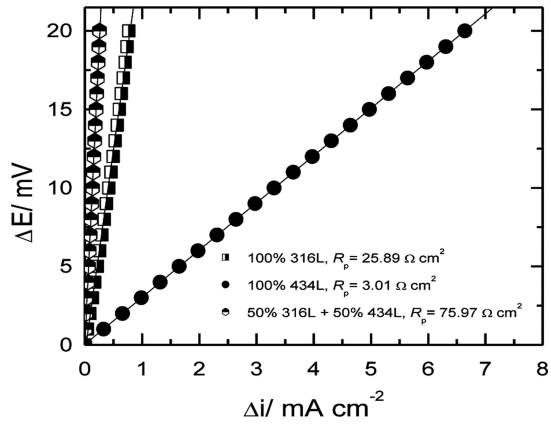

Fig. 7. Changes in external current vs. voltage (within the range of E_{corr} + ΔE) in the analyzed sinters based on potentiokinetic curves recorded for pH = 1

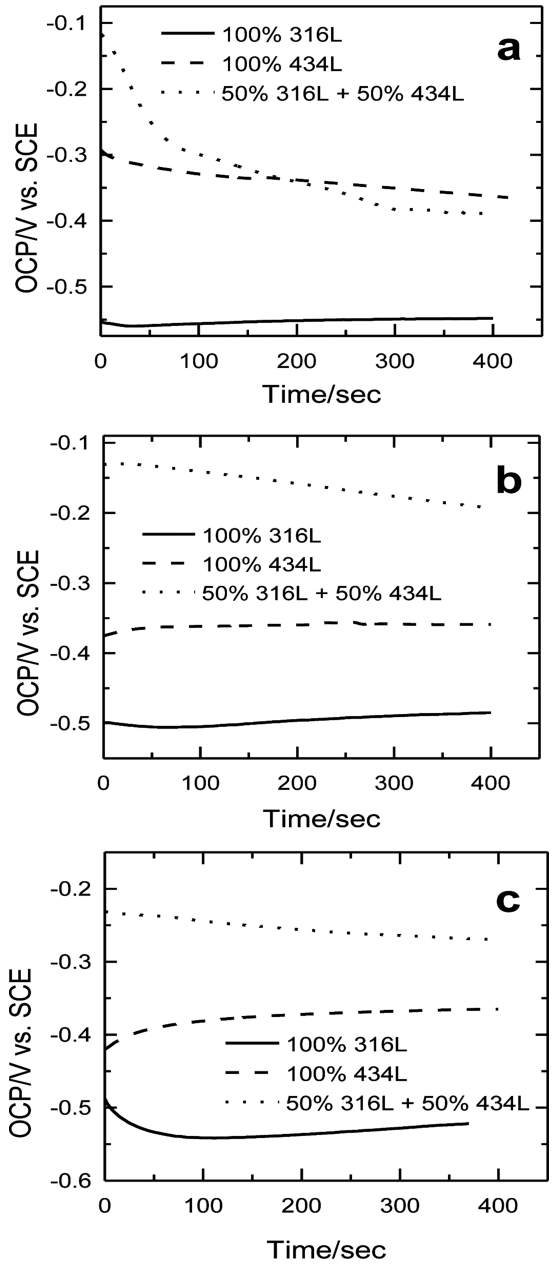

Fig. 8. Open circuit potential of sintered materials in following solutions: a) pH = 1; b) pH = 3; c) pH = 5

5. Summary

- A fundamental condition for categorization of materials as parts in fuel cells is opportunity to obtain materials for the purposes of mass production of this type of electricity generators.
- Powder metallurgy allows for manufacturing of parts with complicated shapes, whereas proper choice of components ensures obtaining materials with the expected functional properties.
- Proper selection of proportions of powders allows for modeling of the structure and properties of the materials obtained by means of powder metallurgy. This operation allows for obtaining alloyed single- and multi-phase steels.
- Modification of martensitic-ferritic steel (434L) through introduction of austenitic steel improves corrosion resistance of the material under the studied conditions, regardless of pH typical of the solution.
- Corrosion resistance of alloyed sintered steel is a function of the type of structure and phase composition of materials.
- Proper evaluation of material resistance under operating conditions of the cell of PEM type in further part of the present investigations will be extended with the investigations of the sinter resistance in the O_2 environment and in the H_2 environment (simulated cathode and anode conditions).

Received: 20 November 2011.

REFERENCES

[1] A. Hermann, T. Chaudhuri, P. Spagnol, Int. J. Hydrogen Energy **30**, 1297 (2005).
[2] J. Larmine, A. Dicks, Fuel cell system explained, Wiley, New York 2000.
[3] H. Tawfik, Y. Hung, D. Mahajan, J. Power Sources **163**, 755 (2007).
[4] A. Kumar, R.G. Reddy, J. Power Source **129**, 62 (2004).
[5] Y. Wang, D.O. Northwood, J. Power Sources **163**, 500 (2006).
[6] Y. Fu, G. Lin, M. Hou, B. Wu, Z. Shao, B. Yi, Int. J. Hydrogen Energy **34**, 405 (2009).
[7] R. Włodarczyk, A. Dudek, Archs. Metall. And Mater. **56**, 797 (2011).
[8] R. Włodarczyk, A. Dudek, Z. Nitkiewicz, Archs. Metall. And Mater. **56**, 180 (2011).
[9] I. Antepara, I. Villarreal, L.M. Rodríguez-Martínez, N. Lecada, U. Castro, A. Leresgoiti, J. Power Sources **151**, 103 (2005).
[10] M. Suliga, Archs. Metall. And Mater. **56**, 823 (2011).
[11] S.-J. Lee, C.-H. Huang, Y.-P. Chen, J. Mat. Proc. Techn **140**, 688 (2003).